Thermal stability, atomic vibrational dynamics, and superheating of confined interfacial Sn layers in Sn/Si multilayers

B. Roldan Cuenya*
Physics Department, University of Central Florida, Orlando, Florida 32816, USA

W. Keune, W. A. Adeagbo, and P. Entel
Fachbereich Physik, Universität Duisburg-Essen, Campus Duisburg, 47048 Duisburg, Germany
(Received 25 July 2005; revised manuscript received 26 September 2005; published 12 January 2006)

Multilayers composed of materials with low (Sn) and high (Si) bulk melting points were grown at room temperature by ultrahigh vacuum deposition. ^{119}Sn Mössbauer spectroscopy has been used to investigate the temperature dependence of the Debye-Waller factor f, the mean-square displacement, and the mean-square velocity of ^{119}Sn nuclei in ultrathin (10 Å thick) α-like Sn layers embedded between 50 Å thick Si layers. The f factor was found to be nonzero with a value of 0.036 ± 0.009 even at 450 °C. This provides unequivocal proof of the solid state of the confined α-like Sn layers at least up to 450 °C. Melting can only be achieved by superheating to $T > 450$ °C. This temperature is significantly higher than the melting temperature of bulk β-Sn (231.9 °C) and of a nonconfined epitaxial α-Sn single layer grown on InSb(111) (170 °C) previously reported in the literature [T. Osaka *et al.*, Phys. Rev. B **50**, 7567 (1994)]. Our molecular dynamics calculations show that melting of bulk-like α-Sn starts at ~380 °C and is complete at ~530 °C according to the Lindemann criterion. Since we still observe the solid state at 450 °C for the confined α-like Sn films, considerable superheating is observed for this system. The stability of the ultrathin confined α-like Sn layers arises from electronic interactions with the surrounding Si layers, as evidenced by the Mössbauer chemical shift.

DOI: 10.1103/PhysRevB.73.045311 PACS number(s): 76.80.+y, 68.60.Dv, 68.65.Ac, 63.50.+x

I. INTRODUCTION

Melting in confined systems is a topical subject. Investigating encapsulated nanocrystals and thin films confined within a higher melting point matrix, previous researchers observed an enhancement of the melting temperature commonly known as "superheating."[1–6] This interesting effect is attributed to the absence of free surface sites and was found be dependent on the thickness of the confined film and on the crystallographic orientation of the host matrix. Recently, molecular dynamics simulations by Akhter[6] on Pb(111) films confined in an Al(111) matrix showed up to 115 K superheating above the bulk melting temperature. This theoretical work is in good agreement with an earlier experimental work by Herman and Elsayed-Ali[7] that reported 120 K superheating on laser-heated Pb(111). A larger enhancement of up to 300 K was calculated by Akhter *et al.* for a Pd(110) film in an Al(111) host.[8] The (110)-to-(111) reorientation of the Pb film embedded in the Al(111) matrix was held responsible for this effect. Thus, melting temperatures obtained from diffraction studies on systems susceptible to reorientation near melting might not be reliable. High-temperature Mössbauer spectroscopy is a powerful technique to investigate these phenomena, provided that the material of interest contains a Mössbauer isotope (i.e., ^{119}Sn). A system can be designed where only the Mössbauer active material is in the confined film, and the onset of melting can be detected by monitoring the disappearance of the Mössbauer signal with increasing temperature.

Metallic β-Sn is a well-studied system with respect to melting of thin films and nanoparticles [T_m(bulk)=232 °C (Ref. 9)]. A size-dependent decrease of the melting point of small isolated or SiO_x-embedded β-Sn nanoparticles with respect to bulk β-Sn has been reported by previous researchers.[10–12] To the best of our knowledge, superheating in encapsulated β-Sn nanoparticles or confined β-Sn films has never been observed. By contrast, the present paper reports the high-temperature stability of the α-Sn phase in ultrathin α-like-Sn films confined by Si layers.

α-Sn is the low temperature Sn phase of semiconducting character with a band gap of 0.08 eV at 300 K and electro-optical properties interesting for infrared device applications.[13,14] Upon heating, Sn undergoes a phase transformation at 13.2 °C from α-Sn (diamond structure, a =6.4798 Å) to β-Sn with double body-centered-tetragonal structure (a=5.83 Å and c=3.18 Å). As a consequence, the melting temperature of bulk α-Sn cannot be measured. However, it is known that α-Sn can be stabilized at $T > 13$ °C by epitaxy on a lattice-matching substrate.

Relatively thick metastable α-Sn layers (2000 Å) can be prepared on InSb(001) (Refs. 15–17) and CdTe(001) (Refs. 18–21) by molecular beam epitaxy (MBE) techniques due to the small lattice mismatch between the film and substrate. On a zinc-blende type of substrate such as CdTe, α-Sn is more stable than β-Sn since the interface can maintain the effective coordination number $Z \approx 4$, which is ideal for both, α-Sn film and substrate.[22] Calculations by Ito *et al.*[22] demonstrate that α-Sn supported on CdTe is more stable than β-Sn by 291 meV/atom at the interface and 628 meV/atom at the thin film regions. Using reflection high-energy electron diffraction techniques (RHEED), Osaka *et al.*[17] observed that 30 ML of α-Sn were stable on InSb(111) beyond 115 °C, and that those films melt at 170 °C directly, without the transition to β-Sn. A chemical bond at the α-Sn/InSb interface

appears to be the most important factor for the stability of α-Sn. They also pointed out that this factor is more important than a smaller lattice misfit, since using crystalline KBr_xCl_{1-x} (a=6.504 Å, x=0.69) as a substrate only leads to β-Sn growth. It appears that in this system a small misfit is a necessary but not a sufficient condition for the onset of α-Sn growth. We have shown previously that up to 3.5 ML (monolayers) of epitaxial metastable α-Sn can be stabilized at RT at the Si(111)-(7×7) surface even under the conditions of a large lattice misfit.[23] A small decrease of the s-electron density at the ^{119}Sn nucleus was found by Mössbauer spectroscopy in sub-monolayers of ^{119}Sn at the Sn/Si(111)-(7×7) interface,[23] very likely due to electronic hybridization of Sn and Si orbitals.

In principle, one can think of determining T_m on a metastable α-Sn single layer. However, the influence of confinement on T_m cannot be determined on epitaxial α-Sn/InSb(001) films. To observe confinement effects one has to embed the α-Sn film between high-T_m thin film materials. We have selected the system Si/Sn/Si for this purpose, because Si is known to have a high T_m of 1412 °C.

Recently, ultrathin (≈10 Å) crystalline α-Sn films[23] and α-like-Sn/a-Si multilayers[24] were successfully grown by MBE at room temperature (RT) on Si(111). The vibrational entropy of crystalline and amorphous α-Sn films was calculated from vibrational density of state curves measured by nuclear resonant inelastic x-ray scattering (NRIXS).[24] The small difference observed ($\Delta S/k_B = +0.17 \pm 0.05$ per atom) could not account for the stability of the α-like-Sn phase in a-Sn/a-Si multilayers. Si-confined α-like Sn films were found to have a significantly higher cutoff phonon frequency than crystalline α-Sn/InSb(001) and β-Sn. The measured Debye temperature of bulk β-Sn [θ_D^{exp} (β-Sn)=195 K (Ref. 25)] is lower than that of bulk α-Sn (θ_D^{exp} (α-Sn)=220 K,[26] and lower than the theoretical values θ_D^{theo} (α-Sn)≃250 K (Ref. 27) and θ_D^{theo} (Si)=613 K (Ref. 28)). The force constants increase in going from Sn to Si. This is consistent with the higher melting point (T_m) for the lighter element, where the average electronic density is higher and the bonds are stronger. Using NRIXS measurements we obtained a larger mean force constant (168±18 N/m) for pure α-like-Sn films in a Sn(10 Å)/Si(50 Å) multilayer as compared to a Sn(20 Å)/Si(50 Å) multilayer (97±20 N/m), where α-like-Sn and β-Sn were found to coexist.[24]

The present paper is organized as follows. In Sec. II we describe experimental details. Section III provides a review of lattice dynamical quantities which are relevant for the evaluation of Mössbauer spectroscopical results. The theoretical background of our molecular dynamics (MD) calculations is briefly described in Sec. IV. Our experimental and theoretical results and the discussion are presented in Sec. V, followed by a summary in Sec. VI.

II. EXPERIMENTAL

Three different Sn/Si mulilayers were prepared. Sample 1 has a composition [^{119}Sn(10 Å)/Si(50 Å)]$_{50}$ and was grown on a polyimid ("kapton") foil in an ultrahigh vacuum (UHV) system. The kapton foil was rinsed in acetone and ethanol just before being loaded into the UHV chamber. Prior to Sn/Si deposition, the kapton foil was heated in UHV to 300 °C for 1 h in order to desorb water from the surface. Sample 2 has a composition [Sn(10 Å)/Si(50 Å)]$_{50}$ and was grown on a MgO(110) wafer under identical conditions as sample 1. The MgO substrate was *ex situ* cleaned with acetone and ethanol and annealed in UHV to 650 °C for 1 h prior to Sn/Si evaporation. Sample 3 has a composition [Sn(10 Å)/Si(50 Å)]$_{43}$ and was deposited on a MgO(110) crystal. The MgO(110) substrate was dipped in boiling concentrated HNO_3 (250 °C) for 10 s and subsequently rinsed in deionized water before loading it into the UHV system. The MgO substrate was heated in UHV to 650 °C for 1 h prior to Sn/Si evaporation. The isotopical enrichment of ^{119}Sn in sample 1 was 82.9%. Sn of natural isotopical composition (8.6% ^{119}Sn) was used for samples 2 and 3.

All multilayers were grown at room temperature (RT). High-purity (undoped) Si was evaporated by an electron gun with a deposition rate of 0.1–0.2 Å/s, and a deposition pressure of $(3-5)\times10^{-9}$ mbar. At first a Si layer was deposited on the kapton foil or MgO(110) wafer, and all multilayers were coated with Si to avoid oxidation. It is known that UHV deposition of Si films under such conditions results in amorphous (a-)Si layers.[24] Metallic ^{119}Sn and natural Sn were evaporated from Knudsen cells (Al_2O_3 crucible) at a deposition pressure of $1-2\times10^{-9}$ mbar and a deposition rate between 0.02 and 0.025 Å/s. The real substrate temperature during deposition was somewhat higher than the previously indicated values, since we measured up to 40 °C by a thermocouple at the sample holder for the RT case. The evaporation rates and film thicknesses were monitored with a calibrated quartz-crystal microbalance and were determined from the bulk density of β-Sn.

^{119}Sn Mössbauer spectroscopy provides information on the structural phase of tin in the multilayers from the ≃0.5 mm/s difference in the center line shifts of bulk α-Sn (δ=2.03±0.02 mm/s at RT) and bulk β-Sn (δ=2.56±0.01 mm/s at RT). Both center-line shift values are relative to a $BaSnO_3$ or $CaSnO_3$ standard absorber.[29,30] For the 23.87 keV Mössbauer γ-radiation ^{119}Sn* in a $CaSnO_3$ matrix was used as source. The Mössbauer spectra were least-squares fitted with the program NORMOS (Ref. 31) with a Lorentzian line shape.

The thermal stability of the interfacial α-like Sn (Ref. 24) in sample 1 was studied *in situ* by means of ^{119}Sn Mössbauer spectroscopy in transmission geometry from RT up to 450 °C. The highest measurement temperature accessible with sample 1 was 450 °C, because the polyimid (kapton) substrate started to decompose at 500 °C in vacuum. A conventional proportional counter was used as detector. For the high-temperature Mössbauer measurements, the sample was inserted in a Mössbauer furnace and was held in high vacuum (1×10^{-5} mbar) by means of a diffusion pump. The sample was clamped at the circumference between two copper plates with a central hole for γ-ray transmission. Sample and sample holder were surrounded with an aluminium foil as a heat shield to maintain a constant and homogenous measurement temperature. The temperature was measured by a

Cromel-Alumel thermocouple fixed on the copper sample holder. A nearly constant reference temperature of 19–21 °C (RT) was measured by another thermocouple located outside of the oven in a water tank. The measurement temperature was automatically regulated by a computer. The accuracy of the sample temperature is estimated to be ±3 °C. The acquisition time per transmission Mössbauer spectrum varied from 1 (RT spectrum) to 11 days (450 °C), depending on the measurement temperature selected. The ^{119}Sn(10 Å)/Si(50 Å) multilayer on MgO(110) (sample 2) was investigated *ex situ* by conversion electron Mössbauer spectroscopy (CEMS) at RT after stepwise isochronal annealing in ultrahigh vacuum (for 1 h) at temperatures from RT up to 500 °C. For CEMS, the sample was placed in a proportional counter filled with a He-4%CH_4 mixture. Θ-2Θ x-ray diffraction (XRD) was performed *ex situ* at RT by using a Cu anode and a graphite monochromator.

III. METHODOLOGICAL ASPECTS

For an isotropic system with lattice vibrations in the harmonic approximation the recoil-energy-free fraction, f, of nuclear resonant absorption events at temperature T (the Debye-Waller factor or Lamb-Mössbauer factor, or simply f factor) and the second-order Doppler shift, δ_{SOD}, at temperature T are given by[32]

$$f(T) = \exp(-k^2\langle x^2\rangle) \tag{1}$$

and

$$\delta_{SOD} = -\langle v^2\rangle/2c. \tag{2}$$

Here, $\langle x^2\rangle$ is the mean-square displacement of the resonantly absorbing nucleus along the γ-ray direction, $\langle v^2\rangle$ is its mean-square velocity, δ_{SOD} is the Doppler velocity (in velocity units) at resonance, c is the velocity of light, and $k = 2\pi/\lambda$ is the wave number of the γ radiation at wavelength λ having energy E_0. (For ^{119}Sn, E_0=23.87 keV, $\lambda = 5.195 \times 10^{-11}$ m, and $k = 1.2095 \times 10^{11}$ m^{-1}.) For an isotropic lattice the mean-square velocity is

$$\langle v^2\rangle = 3\langle v_x^2\rangle, \tag{3}$$

where $\langle v_x{}^2\rangle$ is the mean-square velocity component along the x direction (the γ-ray direction). $\langle v_x{}^2\rangle$ can be accurately obtained, for instance, from the mean kinetic energy $M\langle v_x{}^2\rangle/2$ measured by NRIXS,[24] where M is the mass of the Mössbauer nucleus ($M = 1.975 \times 10^{-25}$ kg for ^{119}Sn).

In the Debye model and for high temperatures $T \geqslant \Theta_D$ (with Θ_D=Debye temperature), the mean-square displacement $\langle x^2\rangle$ depends linearly on temperature[33] according to

$$\langle x^2\rangle = \frac{3\hbar^2}{Mk_B\theta_D^2}T, \tag{4}$$

where k_B is the Boltzmann constant. Then, the high-T approximation of the f factor can be written as

$$f(T) = \exp\left(-\frac{6E_R}{k_B\theta_D^2}T\right), \tag{5}$$

because the free nucleus recoil energy E_R is equal to $p^2/2M = \hbar^2k^2/2M$ ($E_R = 2.57 \times 10^{-3}$ eV for ^{119}Sn). Thus, from the slope s of the $-\ln f$ versus T behavior,

$$-\ln f = \left(\frac{6E_R}{k_B\theta_D^2}\right)T = sT, \tag{6}$$

the Debye temperature is obtained from the relation

$$\Theta_D^2 = \frac{6E_R}{k_B s}. \tag{7}$$

The f factor is known to be proportional to the normalized spectral area A under the absorption versus velocity curve (normalized by the nonresonant count rate) of a Mössbauer spectrum:[34] $f \propto A$ or $f = CA$,

$$-\ln f = -\ln A - \ln C = k^2\langle x^2\rangle. \tag{8}$$

Accordingly, in order to determine the absolute value of the f factor from the experimental spectral area A, the proportionality constant C (or $-\ln C$) must be known, which is often not the case. Usually, one plots measured values of $-\ln A$ vs. T, having Eq. (6) (high-T limit) and Eq. (8) in mind, and one calculates Θ_D from the experimental slope s:

$$s = d(-\ln f)/dT = d(-\ln A)/dT. \tag{9}$$

If the absolute value of f is known from an independent measurement (e.g., from NRIXS) at a certain temperature (e.g., RT), the constant C (or $-\ln C$) in Eq. (8) can be determined from a measurement of A at that temperature. For instance, the value of f=0.21 has been obtained from ^{119}Sn NRIXS on a similar multilayer $[^{119}\text{Sn}(10\ \text{Å})/\text{Si}(50\ \text{Å})]_{50}$ at RT.[24]

The measured shift δ of the center of gravity of a Mössbauer spectrum (the center-line shift or total shift) relative to zero velocity is the sum of two contributions[35]

$$\delta = \delta_{chem} + \delta_{SOD}. \tag{10}$$

Here, δ_{chem} is the chemical shift or isomer shift arising from the electric hyperfine interaction and may be assumed to be independent of T except when a structural or electronic phase transition occurs. δ_{SOD} is the (relativistic) second-order Doppler shift (SOD shift) given (in velocity units) by Eq. (2). δ_{SOD} arises from the lattice vibrations.

For a Debye solid in the high-temperature limit the mean-square velocity $\langle v^2\rangle$ of the Mössbauer nucleus at temperature T is given by[36]

$$\langle v^2\rangle = \frac{3k_BT}{M}\left[1 + \frac{1}{20}\left(\frac{\Theta_D}{T}\right)^2 - \frac{1}{1680}\left(\frac{\Theta_D}{T}\right)^4 + \cdots\right] \tag{11}$$

which for $T \gg \Theta_D$ is reduced to the relation

$$\langle v^2 \rangle = \frac{3k_B T}{M}, \tag{12}$$

resulting in a linear T dependence of δ_{SOD} (and δ) in the classical limit ($T \gg \Theta_D$):

$$\delta_{SOD}(T) = -\frac{3k_B}{2Mc} T. \tag{13}$$

Equation (13) shows that in the classical limit for a given nucleus of mass M, the negative slope of the linear δ_{SOD} vs. T behavior (or linear δ-vs.-T behavior) cannot exceed the value $3k_B/2Mc$. For $T \gg \Theta_D$, δ_{chem} in Eq. (10) may be obtained from the extrapolation of the δ vs. T straight line to $T=0$ K. For ^{119}Sn, the prefactor $-3k_B/2Mc$ in Eq. (13) corresponds to -3.498×10^{-4} (mm/s)/K.

IV. THEORY

In order to investigate the melting of bulk-like α-Sn, molecular dynamic simulations were conducted in the framework of density functional theory (DFT). This was done in combination with the generalized gradient approximation (GGA) for the description of exchange and correlation effects in a functional form proposed by Perdew and Wang as implemented in the Vienna *ab initio* simulation package [VASP (Ref. 37)]. We used $4 \times 4 \times 4$ Monkhorst-Pack[38] k points with energy cutoff of 129.1 eV kept fixed throughout the simulation. The unit cell of the α-Sn structure with lattice parameter 6.489 Å was used.[39] The initial geometry was optimized freely both in shape and volume. However, the relaxed geometry still preserves the diamond structure. In order to determine the stability and transition temperature of the α-Sn structure, constrained molecular dynamics simulations at standard NVT canonical ensemble using the Nosé[40] thermostat were performed. The constrained geometry *ab initio simulation* is a very powerful tool which allows to mimic experimental thin film geometries. Throughout our calculations, the Sn atoms are free to move but the shape, volume, and diamond structure are preserved. The simulation at each temperature run was done for 4000 steps at a time step of 1 fs. The heating was carried out in steps starting from the geometry of the previous temperature run at the interval of 30 K at the lower temperature region, 50 K at the intermediate region, and 100 K in the liquid region. Melting is identified by the inflexion point in the caloric curve (energy-temperature curve, see Sec. V). The average temperature of each run has been determined using the equipartition law from long-time averages of the kinetic energy (E_{kin}),

$$T = \frac{2}{3N-3} \frac{E_{\mathrm{kin}}}{k_B}, \tag{14}$$

where N is the number of degrees of freedom corresponding to the number of Sn atoms (from which the center of mass motion has been removed) and k_B is the Boltzmann constant. As the temperature is increased, the atoms start to vibrate with larger and larger amplitude. Following Lindemann's work,[41] when this amplitude becomes a significant fraction of the equilibrium spacing a between the atoms, melting will occur and the system will undergo a phase transition from an ordered to a disordered state. The mean-square displacement of an atom, $\langle r^2 \rangle$, as a function of temperature is given by

$$\langle r^2 \rangle = \langle |\mathbf{r}(t) - \mathbf{r}(0)|^2 \rangle. \tag{15}$$

Here, $\langle r^2 \rangle$ is the thermal average of the mean square displacement of atoms from their equilibrium lattice position at time t. This expression is connected to the Debye-Waller factor f measured by Mössbauer spectroscopy or NRIXS:

$$f = \exp(-k^2 \langle x^2 \rangle) = \exp(-k^2 \langle r^2 \rangle / 3). \tag{16}$$

According to Lindemann,[41] melting will occur when $\sigma/h = c \approx 0.13 - 0.18$, where $\sigma = \sqrt{\langle r^2 \rangle} = \sqrt{3\langle x^2 \rangle}$ is the root-mean-square displacement, h is the atomic diameter, and the constant $c \approx 0.13$ (≈ 0.18) for fcc-type (bcc-type) materials. Using the lattice parameter $a_0 = 6.489$ Å the unit cell volume $V_0 = a_0^3$ for bulk α-Sn (diamond structure with 8 atoms/unit cell) and the relation $4\pi {r_0}^3/3 = V_0/8$, the Sn atomic diameter in α-Sn can be calculated to be $h = 2r_0 = 4.025$ Å. Accordingly, melting of bulk α-Sn is predicted to occur at $\sigma = \sqrt{3\langle x^2 \rangle} = ch \approx 0.523$ Å or $\langle x^2 \rangle \approx 0.091$ Å^2.

Indeed, as will be shown in Sec. V, the quantity $\langle x^2 \rangle$ shows a rapid increase at the theoretical melting temperature $T_m = 764$ K, which shows that the melting temperature obtained from the results of *ab initio* molecular dynamics simulations performed with the VASP code (caloric curve, see Sec. V) agrees with what is expected from Lindemann's melting criterion. We believe that the theoretical T_m is a trustworthy prediction of the melting temperature of α-Sn, since we have made many simulations of the solid-liquid transition in other systems like water clusters using VASP and other *ab initio* codes (see Ref. 42). In another work by Pavone *et al.*,[43] the α-β transition in tin was simulated using density functional perturbation theory, which shows that calculations based on *ab initio* methods can yield reliable predictions of phase transformations in complex systems such as β-Sn. The free energies of the two phases were computed to be equal to each other at a temperature of 38 °C, in close agreement with the observed transition temperature of ≈ 13 °C.[43]

V. RESULTS AND DISCUSSION

Figure 1 displays transmission ^{119}Sn Mössbauer spectra of the $[^{119}\mathrm{Sn}(10\ \text{Å})/\mathrm{Si}(50\ \text{Å})]_{50}$ multilayer (sample 1) deposited at RT on a kapton foil and measured stepwise *in situ* at RT, 200, 250, 300, 350, and 450 °C, respectively (from top to bottom). All spectra were least-squares fitted with a single Lorentzian line (full line) located close to the resonance velocity for α-Sn.[29,30] The vertical lines indicate the velocity positions of bulk α-Sn (full line) and bulk β-Sn (dashed line) at RT. At RT, sample 1 shows a center-line shift δ of 1.92 ± 0.04 mm/s [Table I (a)], which is close to the bulk α-Sn value [2.03 mm/s (Refs. 29 and 30) in Table I (b)], and in accordance with the center-line shift value of 1.978 ± 0.002 mm/s obtained for a multilayer with the same Sn/Si thicknesses but deposited on Si(111) (see our previous

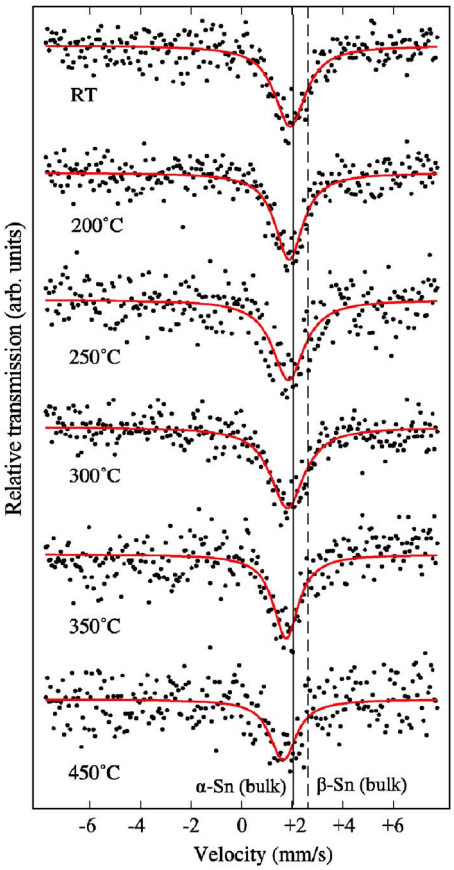

FIG. 1. (Color online) Transmission ^{119}Sn Mössbauer spectra of the $[^{119}\mathrm{Sn}(10\ \text{Å})/\mathrm{Si}(50\ \text{Å})]_{50}$ multilayer on polyimid (kapton) foil (sample 1) measured *in situ* at the indicated temperatures. The measurements were performed by increasing the temperature stepwise from RT to 450 °C. Least-squares fitting (full line) was performed with a single Lorentzian line located close to the velocity position for α-Sn. [The vertical full (dashed) line indicates the velocity position (center line shift) of bulk α-Sn (bulk β-Sn) at RT.]

work, Ref. 24) or on MgO(110) (2.04±0.01 mm/s, Table II). Evidence for the amorphous character of the 10 Å thick α-like ^{119}Sn layer in the Sn/Si multilayers was provided in Ref. 24 by means of x-ray diffraction (XRD) and NRIXS measurements, where the vibrational density of states, $g(E)$, of the interfacial ^{119}Sn layers was obtained. $g(E)$ of the Sn/Si multilayer was found to be significantly different from $g(E)$ of crystalline α-Sn.

Since the melting temperature of bulk β-Sn is ~232 °C,[9] we have measured ^{119}Sn Mössbauer spectra below and above this value to check if the melting point of our amorphous α-like-Sn in the multilayers is similar to that of the bulk β-Sn phase. The pure presence of a Mössbauer signal up to a temperature of 450 °C in Fig. 1 proves unambiguously that the melting temperature of α-like amorphous-Sn in the a-Sn/a-Si multilayers is much higher than that of metallic bulk β-Sn.

Figure 2(a) shows the measured temperature dependence of the center-line shift δ for sample 1 (full circles). The fitted straight line in (a) indicates the classical high-temperature limit ($T \gg \theta_D$) for the second-order Doppler shift according to Eq. (13). (Only the four data points at and below $T=573$ K were included in the least-squares fitting.) At $T=0$ K, the fitted straight line intersects the δ axis at $\delta_{chem}=2.025\pm0.05$ mm/s, according to Eqs. (10) and (13). This value is in good agreement with the chemical shift of bulk α-Sn of 2.03 mm/s reported in the literature [Table I(b)]. With increasing measurement temperature up to 573 K, only a slight decrease in δ was observed as compared to the RT value [Table I (a)]. This linear decrease can be attributed to the second-order Doppler shift. Above 573 K, δ is found to decrease drastically. In this high temperature region, the shift cannot originate exclusively from the second-order Doppler shift. At 623 K, a very low value of δ is measured. We think that the strong reduction of the center-line shift measured at temperatures higher than 523 K indicates a change in the chemical shift, δ_{chem}, due to the onset of interface roughening and/or interfacial atomic intermixing, probably upon crystallization of the Si layers. Independent XRD measurements on similar samples have shown that our 50 Å thick a-Si layers crystallize upon heating at ≈300 °C. Since it is well known that Sn and Si cannot intermix even in the melt,[44] the assumed atomic intermixing is a surface effect and presumably restricted to the interfacial atoms. Further insight into this question will be obtained from RT CEMS performed on a similar multilayer (sample 2) after high-temperature annealing (Fig. 3 and Table II).

By comparing δ values for sample 1 in Table I, which were measured at RT after and before annealing, the following values for the change of the center-line shift $\Delta\delta$, or change of the chemical shift $\Delta\delta_{chem}$ [i.e., $\Delta\delta=\Delta\delta_{chem}=\delta(\text{after annealing})-\delta(\text{before annealing})$, measured at RT] have been obtained: $\Delta\delta=-0.11$ mm/s for 350 °C, and −0.08 mm/s for 450 °C annealing.

The chemical shift δ_{chem} is proportional to the total s-electron density at the nucleus, $|\psi(0)|^2$. The anomalous decrease in $\delta=\delta_{chem}+\delta_{SOD}$ (with respect to the classically predicted high-temperature linear behavior) obtained for the interfacial α-like-Sn films at $T>573$ K [Fig. 2(a)] is equivalent to a reduction $\Delta|\psi(0)|^2$ of the s-electron density at the Sn nucleus by $\approx 0.546\pm0.006\ a_0^{-3}$ at $T=623$ K and $\approx 1.42\pm0.03\ a_0^{-3}$ at $T=723$ K (a_0=Bohr radius), as obtained from

$$\Delta|\psi(0)|^2=\Delta\delta/\alpha, \tag{17}$$

where $\alpha=0.086\ a_0^3$ mm/s for ^{119}Sn,[45] and $\Delta\delta=\Delta\delta_{chem}=-0.047\pm0.001$ mm/s and -0.122 ± 0.002 mm/s at 623 K and 723 K, respectively, relative to the straight line [Fig. 2(a)].

Figure 2(b) displays the measured quantity $-\ln A$ versus the measurement temperature T for sample 1, where A is the relative spectral area of the α-Sn-like phase. (The nonresonant intensity has been used as normalization factor.) The straight line in Fig. 2(b) is a least-squares fit to the data points in agreement with Eqs. (6) and (8),

$$-\ln A=C_1+C_2\cdot T=C_1+\left(\frac{6E_R}{k_B\cdot\theta_D^2}\right)T. \tag{18}$$

TABLE I. (a) Temperature dependence of the ^{119}Sn Mössbauer parameters [center-line shift δ (measured by using the $CaSnO_3$ source) and linewidth Γ (FWHM) of the Lorentzian line] of [^{119}Sn(10 Å)/Si(50 Å $]_{50}$ deposited on a polyimid (kapton) foil (sample 1). The data are extracted from Fig. 1. Mössbauer parameters (center-line shift and linewidth at room temperature, RT) of epitaxial α-^{119}Sn(500 Å)/InSb(001) (Ref. 24), of α-^{119}Sn(10 Å)/Si(111) (Ref. 23), and of a β-Sn foil (Ref. 23), all measured at RT, and comparison with the crystalline bulk values taken from the literature.[29,30] (*) represents a parameter held fixed for fitting.

(a) Sample 1 [Sn(10 Å)/Si(50 Å $]_{50}$ on Kapton foil	Center-line shift δ(mm/s)		Lorentzian linewidth Γ(mm/s)	
Measurement temperature T(°C)	α-like-Sn	β-Sn	α-like-Sn	β-Sn
RT	1.92±0.04		1.5±0.1	
200 °C	1.881±0.003		1.33±0.01	
250 °C	1.86±0.03		1.49±0.09	
300 °C	1.81±0.01		1.60±0.04	
350 °C	1.76±0.02		1.2±0.06	
450 °C	1.65±0.03		1.3±0.1	
RT after anneal to 350 °C	1.81±0.03		1.40±0.09	
RT after anneal to 450 °C	1.84±0.03	2.56±0.07	1.5(*)	0.9±0.2
(b) T=RT	α-Sn	β-Sn	α-Sn	β-Sn
α-Sn(500 Å)/InSb(001) (Ref. 24)	1.99±0.01		0.924±0.004	
α-Sn(10 Å)/Si(111) (Ref. 23)	2.07±0.02		1.41±0.007	
α-Sn (bulk) (Refs. 29 and 30)	2.03±0.02			
β-Sn (foil) (Refs. 16 and 24)		2.520±0.002		0.854±0.004
β-Sn (bulk) (Refs. 29 and 30)		2.56±0.01		

The linear fit results in $C_1=4.4\pm0.1$ and $C_2=(0.004\,09\pm0.0002)\ K^{-1}$. A Debye temperature of 209±5 K can be obtained using the value of the recoil energy of the ^{119}Sn emitting nucleus, $E_R=2.572$ meV.[46] This value is somewhat higher than the Debye temperature measured by Corak and Satterthwaite[25] for β-Sn ($\theta_D^{exp}=195$ K), but lower than the value obtained by Hill and Parkinson[26] for crystalline α-Sn ($\theta_D^{exp}=220$ K). In a theoretical and experimental study on lattice dynamics of substitutional ^{119}Sn in Si, Ge, and α-Sn, Petersen *et al.*[47] reported $\theta_D^{exp}=161$ K for ^{119}Sn in

TABLE II. ^{119}Sn Mössbauer parameters [center-line shift δ (measured by using the $CaSnO_3$ source), linewidth Γ (FWHM) of the Lorentzian line, and relative spectral area A] measured at RT after stepwise isochronal annealing treatments (1 h) of a [Sn(10 Å)/Si(50 Å $]_{50}$ multilayer deposited on MgO(110) (sample 2). The data are extracted from Fig. 3. (*) represents a parameter held fixed for fitting.

Sample 2 [Sn(10 Å)/Si(50 Å $]_{50}$ on MgO(110)	Center-line shift δ(mm/s) at RT		Lorentzian linewidth Γ(mm/s) at RT		Area (%)	
Annealing temperature T(°C)	α-like-Sn	β-Sn	α-like-Sn	β-Sn	α-like-Sn	β-Sn
RT	2.04±0.01		1.17±0.05		100	
200 °C	2.05±0.01		1.29±0.04		100	
250 °C	2.08±0.01		1.25±0.04		100	
300 °C	2.017±0.009		1.18±0.03		100	
355 °C	1.95±0.01		1.17±0.03		100	
400 °C	1.895±0.008	2.56(*)	0.96±0.02	1.06±0.008	81±2	19±2
450 °C	1.87±0.01	2.56(*)	0.91±0.05	1.5±0.2	75±4	25±5
500 °C	1.87±0.02	2.56(*)	0.92±0.05	1.1±0.2	79±5	21±5

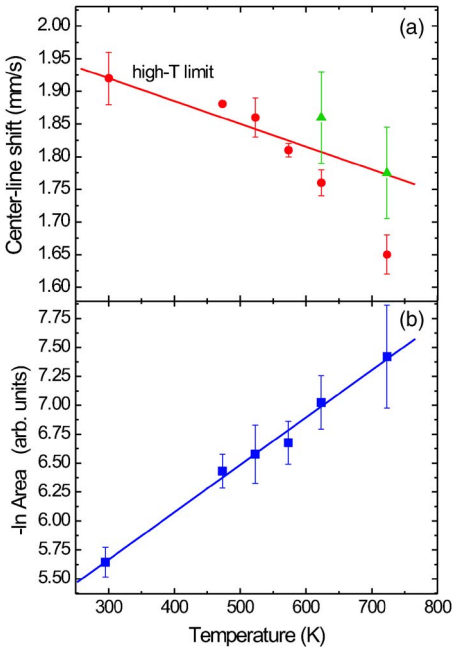

FIG. 2. (Color online) (a) Measured T dependence of the center-line shift δ (full circles) obtained from Fig. 1. The straight line in (a) indicates the (classical) high-T limit, $T \gg \theta_D$ (θ_D=Debye temperature) for the second-order Doppler shift (SOD) according to Eq. (13). Full triangles: high-T data points corrected for the decrease in the chemical shift $\Delta\delta_{chem}=\Delta\delta$ measured at RT before and after annealing to 350 °C and 450 °C, respectively, according to Table I. (b) Measured T dependence of $-\ln A$ obtained from Fig. 1. (A being the relative spectral area of the α-Sn line normalized with the nonresonant intensity.) The straight line is a least-squares fit to the data points, according to Eqs. (6) and (8), resulting in θ_D=209 K.

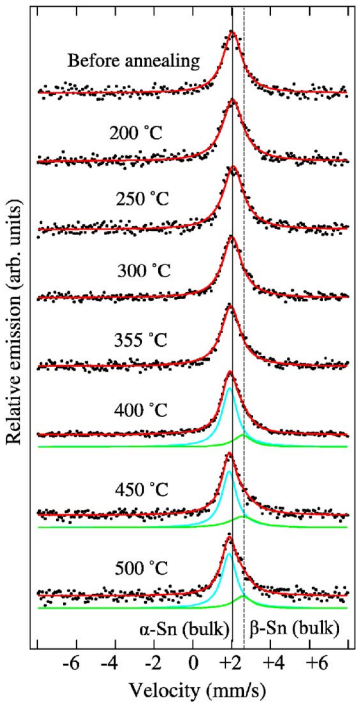

FIG. 3. (Color online) ^{119}Sn CEM spectra of $[\mathrm{Sn}(10\ \text{Å})/\mathrm{Si}(50\ \text{Å})]_{50}$ multilayer on MgO(110) (sample 2) measured *ex situ* at RT after isochronal annealing (1 h) at the indicated temperatures. The sample was annealed stepwise from RT to 500 °C. The full line through the data points is a least-squares fit with one Lorentzian line for α-Sn (RT to 355 °C) or with two Lorentzian lines for α-Sn and β-Sn, respectively (400 °C to 500 °C). The vertical full (dashed) line indicates the velocity position (center-line shift) of bulk α-Sn (bulk β-Sn) at RT.

α-Sn and θ_D^{exp}=223 K for ^{119}Sn in Si. These values were obtained from Debye curve fits to the temperature dependence of the relative f factors measured by ^{119}Sn Mössbauer spectroscopy. Our experimentally determined Debye temperature lies between these latter values, suggesting that some interfacial intermixing/interface roughening might have occurred in our samples. Alternatively, the differences measured can also be attributed to the amorphous nature of our ultrathin α-like-Sn films.

The CEM spectra shown in Fig. 3 were obtained from sample 2, which is similar to sample 1 but was deposited on MgO(110). These spectra were all measured at RT before and after stepwise isochronal annealing up to 500 °C (from top to bottom). Similarly to Fig. 1, the spectra were least-squares fitted with a single Lorentzian line (from RT to 350 °C) or with a superposition of two Lorentzian lines, i.e., a dominant one for α-Sn and a minor one for β-Sn (from 400 to 500 °C). The center-line shift δ of the multilayer measured *ex situ* at RT after 1 h annealing remains unchanged up to an annealing temperature of 300 °C (Fig. 3). After annealing at 355 °C and subsequent cooling to RT, a small decrease in the center-line shift can be observed (see Table II), but the spectrum can still be fitted with a single Lorentzian line with a center-line shift close to that of bulk α-Sn. After further annealing (400 to 500 °C) and subsequent RT cooling (Fig. 3, bottom), the CEM spectrum had to be fitted by the superposition of two Lorentzian lines, indicating the coexistence of a large fraction of α-Sn and a small fraction of β-Sn (see also the relative spectral areas given in Table II).

The slightly lower center-line shifts δ obtained from RT Mössbauer spectra after annealing sample 2 to temperatures >300 °C (Table II) are in fair agreement with the Mössbauer results on sample 1 (Table I). For sample 2 at RT, the measured difference $\Delta\delta=\Delta\delta_{chem}=\delta$(after annealing) $-\delta$(before annealing) is found to be −0.09 mm/s for 355 °C annealing and −0.17 mm/s for 450 °C annealing (Table II). For sample 1 at RT, the corresponding values are −0.11 mm/s after 350 °C annealing and −0.08 mm/s after 450 °C annealing. The measured $\Delta\delta_{chem}$ values averaged over the two samples are −0.1 mm/s after ~350 °C annealing and −0.125 mm/s after 450 °C annealing. In Fig. 2(a), the high-T data points for δ at 623 K (350 °C) and 723 K (450 °C) have been corrected for their corresponding average $\Delta\delta_{chem}$ values, yielding the two corrected data points (full triangles) in Fig. 2(a). The high-T limit (straight line) in Fig. 2(a) provides a good approximation to the data over the whole temperature regime, including the two corrected high-T data points.

According to previous Mössbauer data on substitutional ^{119}Sn in α-Sn (δ=1.97 mm/s), β-Sn (δ=2.56 mm/s), and crystalline-Si (δ=1.74 mm/s),[13] the RT center-line shift of

the 450 °C annealed α-like-Sn/a-Si multilayers (1.84 mm/s for sample 1 and 1.87 mm/s for sample 2) lies between the RT values of ^{119}Sn diluted in c-Si and pure α-Sn. Moreover, our RT δ values are significantly larger than the center-line shifts reported by Fanciulli *et al.*[48] ($\sim$1.72–1.74 mm/s at RT) for Sn in $Si_{1-x}Sn_x$ pseudomorphic layers grown on Si(001) by MBE. We conclude that the interfacial ^{119}Sn electronic state in our multilayers after annealing is not comparable to that in metastable $Si_{1-x}Sn_x$ layers and in ^{119}Sn-doped c-Si, where the average ^{119}Sn atoms are surrounded by Si nearest neighbors in the diamond structure. We assume that at the same temperature (RT) the total shift δ (or chemical shift δ_{chem}) is proportional to the number of Si nearest neighbors around the ^{119}Sn atom. Taking a value of δ = 2.03 mm/s for ^{119}Sn in bulk α-Sn (zero Si neighbors, Z = 0) and δ = 1.74 mm/s for dilute ^{119}Sn in c-Si (Z=4 Si neighbors), we can estimate from δ = 1.84 mm/s an average number of Si neighbors Z in our interfacial ^{119}Sn layer of about 2.6. This may be compared with the case of an atomically sharp coherent (001)Sn/Si interface (diamond structure), where we find Z=2. The estimated weak increase of ΔZ=0.6 in the average number of Si neighbors at the Sn/Si interfaces in our multilayers due to annealing provides an argument for rather weak atomic intermixing and modest topological interface roughness in the Sn/Si interfacial region.

Williamson *et al.*[14] observed that annealing of amorphous hydrogenated $Si_{1-x}Sn_x$ multilayers with $x \simeq 0.3-0.4$ at a critical temperature of 400 °C under N_2-10% H_2 resulted in β-Sn precipitation, H_2 evolution, and partial crystallization of the a-Si matrix. We know from XRD data on multilayers similar to ours that crystallization of our thin a-Si films in the multilayers upon annealing occurs at $\approx$300 °C. Therefore, the anomalous drop in the center-line shift at temperatures higher than 300 °C ($\sim$573 K) in Fig. 2(a) appears to be related to recrystallization of Si and, most likely, also of the amorphous α-like-Sn layers. It is very likely that interface roughening and/or interfacial intermixing is correlated with the amorphous-to-crystalline transition. This is shown in Fig. 4 for sample 3, a Sn/Si multilayer deposited on MgO(110) and subsequently stepwise isochronally annealed (1 h) in high vacuum from RT up to 500 °C. In the as-grown state and up to 250 °C, no Bragg reflections of the multilayer are visible, indicating the amorphous state of Si and Sn, in agreement with the results in Ref. 24. The crystallization of the Si layers at $\approx$300 °C is indicated by the appearance of the Si(111) and (220) reflections. Furthermore, above 500 °C, XRD peaks corresponding to crystalline β-Sn can be observed. However, no signal of crystalline α-Sn could be detected by XRD, indicating that the α-like Sn phase (which is still present after 500 °C annealing according to the CEM spectrum in Fig. 3) very likely remains amorphous or disordered. We would like to emphasize that the small fraction of β-Sn forming at and above 400 °C will not provide a Mössbauer signal in Fig. 1, because β-Sn will be in the liquid state at such high temperatures.

As previously mentioned, the Debye-Waller factor f is proportional to the Mössbauer spectral area A, Eq. (8). The proportionality constant was obtained using the known (absolute) f factor (f=0.21) determined from NRIXS measurements at RT on a similarly prepared α-like-Sn(10 Å)/a-Si multilayer.[24] This constant has been used to normalize the spectral areas measured by transmission Mössbauer spectroscopy at the higher measurement temperatures.

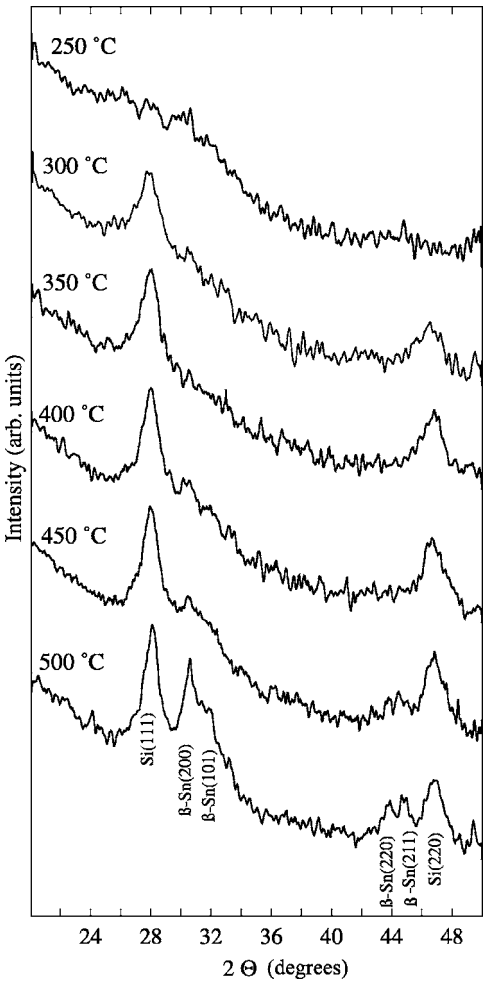

FIG. 4. X-ray diffractometry scans (Θ-2Θ) of a $[^{119}Sn(10\ Å)/Si(50\ Å)]_{43}$ multilayer deposited on MgO(110) (sample 3). The XRD scans were recorded *ex situ* at RT after stepwise isochronal annealing (1 h) from RT to 500 °C. The observed Bragg peaks of Si and β-Sn are indicated (λ_{K_α} = 1.541 78 Å).

Figure 5(a) displays the temperature dependence of the (absolute) Debye-Waller factor f (full circles) obtained from the Mössbauer data in Fig. 2(b), from NRIXS at 300 K for epitaxial crystalline α-Sn/InSb (Ref. 24) (cross), β-Sn (Ref. 49) (full triangle), and from the present molecular dynamics simulations (open squares). The theoretical f-factor values calculated for bulk-like crystalline α-Sn are overall somewhat smaller than the ones determined experimentally for the confined α-like Sn layers. In particular, the RT f factor obtained from theory is closer to the value of β-Sn obtained from NRIXS experiments.[21]

Figure 5(b) shows the mean-square displacement $\langle x^2 \rangle$ of the ^{119}Sn Mössbauer atom (full circles) obtained from the measured Debye-Waller factor [Fig. 5(a)] (full circles) and obtained from the present MD simulations for crystalline α-Sn (open squares). The RT $\langle x^2 \rangle$ values obtained from

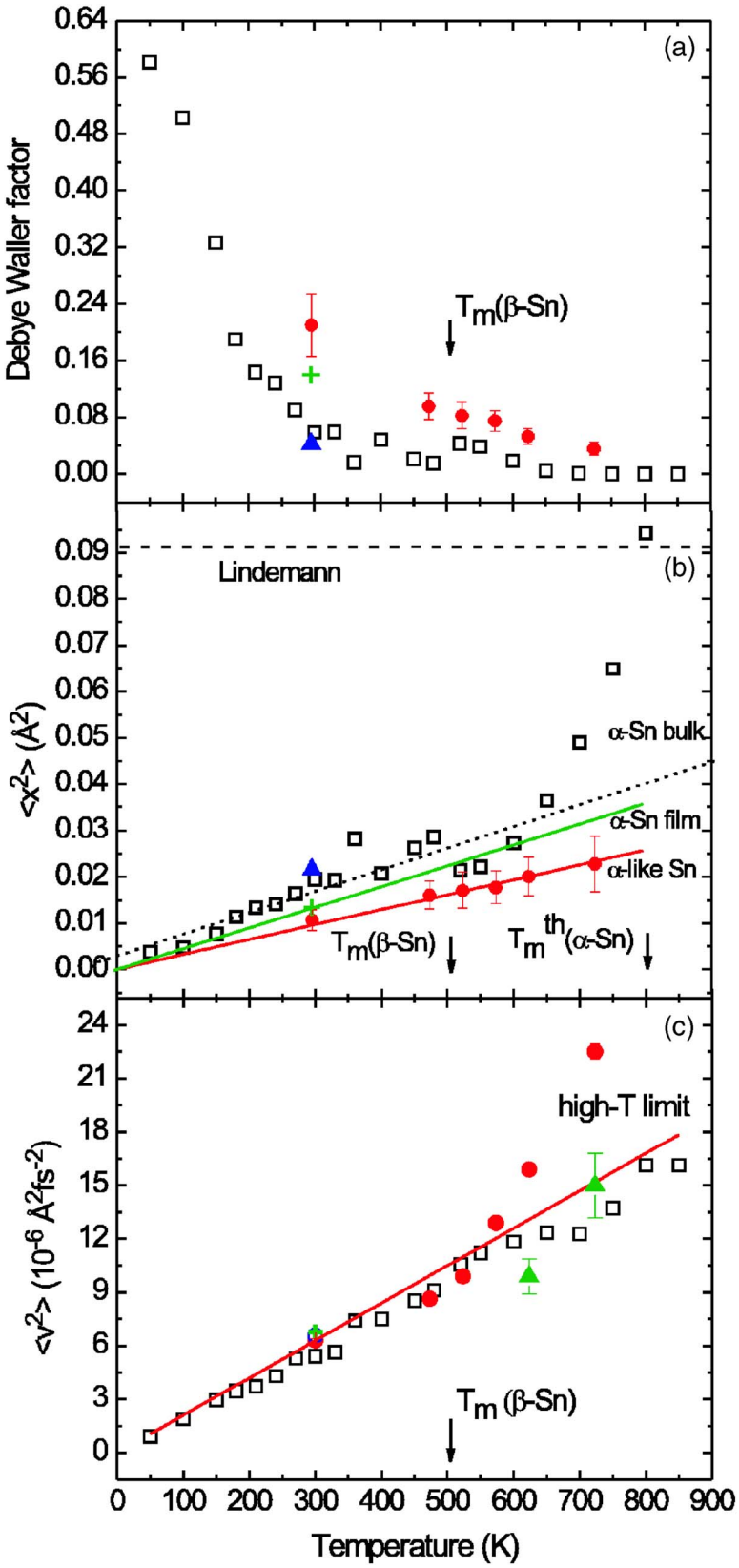

FIG. 5. (Color online) Temperature dependence of (a) the ^{119}Sn Debye-Waller factor (f factor) of confined α-like Sn obtained from the Mössbauer data in Fig. 2(b) (full circles), from NRIXS at 300 K for epitaxial α-Sn/InSb (Ref. 24) (cross) and β-Sn (Ref. 49) (full triangle), and from the present theory (open squares). The Mössbauer data were normalized to $f=0.21$ at 300 K obtained by NRIXS (Ref. 24) on a $[^{119}\mathrm{Sn}(10\ \text{Å})/\mathrm{Si}(50\ \text{Å})]_{50}$ multilayer on Si(111). (b) Mean square displacement $\langle x^2\rangle$ of the ^{119}Sn Mössbauer atom obtained from the experimental f factor [(a)] (full circles), from NRIXS at 300 K for epitaxial α-Sn/InSb (Ref. 24) (cross), for β-Sn (Ref. 49) (full triangle), and from the present theory (open squares). The upper straight line (dotted) is a least-squares-fit of our theoretical results for temperatures below 650 K. The middle straight line indicates the classical behavior ($T \gg \theta_D$) for epitaxial α-Sn/InSb ($\theta_D=165.1$ K), while the lower straight line is a least-squares fit to the present Mössbauer data (full circles), indicating classical behavior. The horizontal dashed line indicates $\langle x^2\rangle$ according to the Lindemann theorem, where melting occurs. (c) Mean-square velocity $\langle v^2\rangle$ of the ^{119}Sn atom obtained from the Mössbauer data in Fig. 2(a) (full circles). Full triangles: corrected $\langle v^2\rangle$ values at high T, obtained from the corresponding corrected data points in Fig. 2(a) (full triangles). The straight line indicates the classical high-T limit for the second-order Doppler shift (δ_{SOD}) according to Eq. (13). Data obtained from NRIXS at 300 K for epitaxial α-Sn/InSb (Ref. 24) (cross) and amorphous α-like Sn (Ref. 24) (open circle), and from the present theory (open squares), are also plotted. T_m (β-Sn) is the experimental melting temperature of bulk β-Sn, while T_m^{th}(α-Sn) is the theoretical melting temperature of bulk α-Sn according to the present theory and the Lindemann theorem.

NRIXS on epitaxial α-Sn/InSb (Ref. 24) (cross) and β-Sn (Ref. 49) (full triangle) are also displayed. The middle straight line indicates the classical behavior ($T \gg \theta_D$) for an epitaxial α-Sn film on InSb ($\theta_D=165.1$ K), while the lower straight line is a least-squares fit to the present experimental data (full circles), indicating classical behavior. It can be observed that the mean-square displacements of the Sn atoms in the Si-confined α-like-Sn layers are smaller than those of

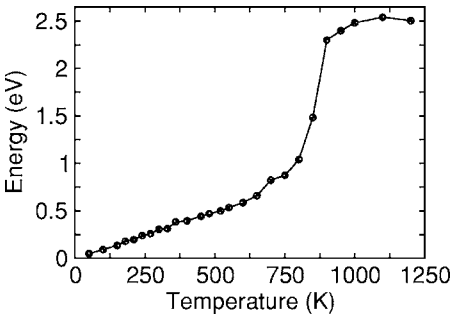

FIG. 6. Energy versus temperature plot for α-Sn as obtained from *ab initio* molecular dynamics simulations using VASP. The simulation at each temperature was done for 4000 steps with a time step of 1 fs. The last 2000 steps were used for calculation of average quantities. The rather sudden increase of the caloric curve is a hint of melting.

Sn atoms in crystalline unconfined α-Sn films and bulk α-Sn.

The theoretical $\langle x^2 \rangle$ values [Fig. 5(b), open squares] calculated for bulk crystalline α-Sn are overall larger than our experimental data and show a drastic increase above 650 K. The upper straight line in Fig. 5(b) (dotted line) represents a least-squares fit of the theoretical results below this critical temperature. Above 650 K, a strong nonlinear increase of $\langle x^2 \rangle$ with temperature is observed. This change is associated with the onset of the solid-to-liquid phase transition of bulk α-Sn. Following Lindemann's criterion, complete melting of bulk α-Sn is theoretically predicted at a temperature of about 800 K, which shows that the melting temperature obtained from the results of *ab initio* molecular dynamics simulations performed with the VASP code (caloric curve in Fig. 6) agrees with what is expected from Lindemann's melting criterion. By contrast, melting has not been experimentally observed for our confined α-like-Sn layers in that temperature range, because we could measure transmission Mössbauer spectra (solid phase) of α-like interfacial Sn up to 723 K. This demonstrates that the surprisingly high thermal stability of our α-like films is due to the confinement by the surrounding Si layers.

The mean-square velocity $\langle v^2 \rangle$ of the ^{119}Sn Mössbauer atom obtained from the present Mössbauer data [Fig. 2(a)] is displayed in Fig. 5(c) (full circles). These data were extracted from the temperature-dependent total center-line shift $[\delta(T) = \delta_{chem} + \delta_{SOD}(T)]$ and make use of the proportionality of δ_{SOD} and $\langle v^2 \rangle$, Eq. (2). In the present work, $\langle v^2 \rangle = 2c \times (2.025\ \mathrm{mm/s} - \delta)$, according to Eqs. (2) and (10).

The straight line in Fig. 5(c) indicates the classical high-temperature limit $T \gg \theta_D$ for the second-order Doppler shift (δ_{SOD}) according to Eq. (12). Data obtained from NRIXS at 300 K for epitaxial α-Sn/InSb (Ref. 24) (cross) and amorphous α-like Sn (Ref. 24) (open circle) and from the present theory (open squares) are also plotted. The experimental mean-square velocities of the Sn atoms in the confined α-like-Sn layers are in agreement with the ones calculated by molecular dynamics for crystalline bulk α-Sn over the entire temperature range. Our experimental data follow the high-temperature approximation for $\langle v^2 \rangle$ from RT up to 600 K. The drastic increase of the experimental $\langle v^2 \rangle$ values above 600 K which exceeds the high-T limit (full circles) is not due to the second-order Doppler shift, but is an artifact of changes in δ_{chem}. If we use the corrected δ values at 623 K and 723 K (full triangles) in Fig. 2(a) for the calculation of $\langle v^2 \rangle$, we obtain the corrected $\langle v^2 \rangle$ values at 623 K and 723 K (full triangles) in Fig. 5(c). The latter values are reasonably well described by the straight-line (high-T limit) in Fig. 5(c).

Figure 6 shows a caloric curve for bulk α-Sn obtained from *ab initio* molecular dynamics simulations using VASP. The increase of the energy versus T curve around 764 K goes hand in hand with the onset of melting of a substantial part of the system. For a better fixing of the melting temperature, a larger number of atoms must be used in order to obtain smoother heating and cooling (not calculated here) $E(T)$ curves.

VI. SUMMARY

We have investigated multilayers composed of materials with a low (Sn) and high (Si) melting point, T_m, in the bulk. The temperature dependence of the Debye-Waller factor, the mean-square displacement, and the mean-square velocity of ^{119}Sn nuclei in ultrathin (10 Å thick) α-like Sn layers embedded between 50 Å thick Si layers has been measured by ^{119}Sn Mössbauer spectroscopy in the temperature range between 20 °C and 450 °C. The multilayer was grown at RT by ultrahigh vacuum deposition. Even at 450 °C the f factor was found to be nonzero with a value of 0.036 ± 0.009 corresponding to $\langle x^2 \rangle = (0.023 \pm 0.006)$ Å^2. This proves unambiguously that the confined α-like Sn layers are in the solid state at least up to 450 °C, and melting can only be achieved by superheating to $T > 450$ °C. Hence, the melting temperature of confined α-like Sn is significantly higher than T_m of bulk β-Sn (231.9 °C) and of a nonconfined epitaxial α-Sn single layer on InSb(111) ($T_m = 170$ °C) reported in the literature.[17] Molecular dynamics calculations demonstrate that the melting of bulk-like α-Sn starts at ~380 °C and is complete at ~530 °C according to the Lindemann criterion. Since we still observe the solid state at 450 °C for the confined α-like Sn layers, considerable superheating exists for this confined system as compared to the calculated T_m for bulk-like α-Sn. The stability of the ultrathin confined α-like Sn layers arises from electronic interactions with the surrounding Si layers in the interfacial region, as evidenced by the Mössbauer chemical shift.

ACKNOWLEDGMENTS

We are very grateful to Ulrich von Hörsten for his expertise technical assistance and to Dr. Alexey Zayak for helpful discussions. Work financially supported by Deutsche Forschungsgemeinschaft (GK 277 and SFB 491).

*E-mail: roldan@physics.ucf.edu

[1] Z. H. Jin, H. W. Sheng, and K. Lu, Phys. Rev. B **60**, 141 (1999).
[2] K. Lu and Y. Li, Phys. Rev. Lett. **80**, 4474 (1998).
[3] L. Zhang, Z. H. Jin, L. H. Zhang, M. L. Sui, and K. Lu, Phys. Rev. Lett. **85**, 1484 (2000).
[4] Q. Jiang, L. H. Liang, and J. C. Li, J. Phys.: Condens. Matter **13**, 565 (2001).
[5] Q. Jiang, Z. Zhang, and J. C. Li, Chem. Phys. Lett. **322**, 549 (2000).
[6] J. I. Akhter, J. Phys.: Condens. Matter **17**, 53 (2005).
[7] J. W. Herman and H. E. Elsayed-Ali, Phys. Rev. Lett. **69**, 1228 (1992).
[8] J. I. Akhter, Z. H. Jin, and K. Lu, J. Phys.: Condens. Matter **13**, 7969 (2001).
[9] *Metals Handbook*, edited by T. Lyman (ASM, Metals Park, OH, 1948).
[10] T. Bachels, H. J. Güntherodt, and R. Schäfer, Phys. Rev. Lett. **85**, 1250 (2000).
[11] S. L. Lai, J. Y. Guo, V. Petrova, G. Ramanath, and L. H. Allen, Phys. Rev. Lett. **77**, 99 (1996).
[12] C. E. Bottani, A. Li Bassi, A. Stella, P. Cheyssac, and R. Kofman, Europhys. Lett. **56**, 386 (2001).
[13] D. L. Williamson and S. K. Deb, J. Appl. Phys. **54**, 2588 (1983).
[14] D. L. Williamson, R. C. Kerns, and S. K. Deb, J. Appl. Phys. **55**, 2816 (1984).
[15] B. Roldan Cuenya, M. Doi, O. Marks, W. Keune, and K. Mibu, "Reflection High-Energy Electron Diffraction and ^{119}Sn Mössbauer investigations of epitaxial α-Sn Films," in *Structure and Dynamics of Heterogeneous Systems*, edited by P. Entel and D. E. Wolf (World Scientific, Singapore, 2000), p. 251.
[16] B. Roldan Cuenya, "Magnetism, structure and vibrational dynamics of nanoscaled heterostructures: interfaces, ultrathin films and multilayers," dissertation, Gerhard-Mercator-Universität Duisburg, Duisburg, Germany, 2001.
[17] T. Osaka, H. Omi, K. Yamamoto, and A. Ohtake, Phys. Rev. B **50**, 7567 (1994).
[18] L. W. Tu, G. K. Wong, and J. B. Ketterson, Appl. Phys. Lett. **54**, 1010 (1989).
[19] H. Zimmerman, R. C. Keller, P. Meisen, and M. Seelmann-Eggebert, Surf. Sci. **377-379**, 904 (1997).
[20] A. Dittmar-Wituski and P. J. Moller, Surf. Sci. **287**, 577 (1993).
[21] M. Y. Hu, "Inelastic Nuclear Resonant Scattering and Its Applications to Tin Materials," Ph.D. thesis, Northwestern University, Evanston, IL, 1999.
[22] T. Ito, J. Appl. Phys. **31**, L920 (1992).
[23] B. Roldan Cuenya, M. Doi, and W. Keune, Surf. Sci. **506**, 33 (2002).
[24] B. Roldan Cuenya, W. Keune, W. Sturhahn, T. S. Toellner, and M. Y. Hu, Phys. Rev. B **64**, 235321 (2001).
[25] W. S. Corak and C. B. Satterthwaite, Phys. Rev. **102**, 662 (1956).
[26] R. W. Hill and D. H. Parkinson, Philos. Mag. **43**, 309 (1952).
[27] M. S. Kushwaha, Physica B **101**, 254 (1980).
[28] K. J. Chang and M. L. Cohen, Phys. Rev. B **34**, 4552 (1986).
[29] A. Svane, N. E. Christensen, C. O. Rodriguez, and M. Methfessel, Phys. Rev. B **55**, 12572 (1997).
[30] *Mössbauer Effect Data Index Covering the 1974 literature*, edited by J. G. Stevens and V. E. Stevens (IFI/Plenum, New York, 1975), p. 153.
[31] R. A. Brand, Nucl. Instrum. Methods Phys. Res. B **28**, 417 (1987).
[32] R. D. Taylor and P. P. Craig, Phys. Rev. **175**, 782 (1968).
[33] G. Schatz and A. Weidinger, *Nukleare Festkörperphysik* (Teubner, Stuttgart, 1992), p. 53 (in German).
[34] D. A. Shirley, M. Kaplan, and P. Axel, Phys. Rev. **123**, 816 (1961).
[35] D. Barb, *Grundlagen und Anwendungen der Mössbauerspektroskopie*, edited by W. Meisel (Akademie-Verlag, Berlin, 1980), p. 151 (in German).
[36] G. K. Shenoy, F. E. Wagner, and G. M. Kalvius, "The Measurement of Isomer Shifts," in *Mössbauer Isomer Shifts*, edited by G. K. Shenoy and F. E. Wagner (North-Holland, Amsterdam, 1978), p. 49.
[37] G. Kresse and J. Furthmüller, Phys. Rev. B **54**, 11169 (1996).
[38] H. J. Monkhorst and J. D. Pack, Phys. Rev. B **13**, 5188 (1976).
[39] P. Villars and L. D. Calvert, *Pearson's Handbook of Crystalline Data for Intermetallic Phases* (American Society for Metals, Metals Park, OH, 1991).
[40] S. Nosé, J. Chem. Phys. **81**, 511 (1984).
[41] F. A. Lindemann, Z. Phys. **11**, 609 (1910).
[42] W. A. Adeagbo and P. Entel, Phase Transitions **77**, 63 (2004).
[43] P. Pavone, S. Baroni, and S. de Gironcoli, Phys. Rev. B **57**, 10421 (1998).
[44] M. Hansen and K. Anderko, *Constitution of Binary Alloys* (McGraw-Hill, New York, 1958).
[45] M. Grodzicki, V. Männing, A. X. Trautwein, and J. M. Friedt, J. Phys. B **20**, 5595 (1987).
[46] D. Niemeier, H. Mehner, U. Bismayer, and K. D. Becker, Phys. Status Solidi B **211**, 581 (1999).
[47] J. W. Petersen, O. H. Nielsen, G. Weyer, E. Antoncik, and S. Damgaard, Phys. Rev. B **21**, 4292 (1980).
[48] M. Fanciulli, H. C. Vestergaard, G. Weyer, M. Fyhn, S. Yu Shiryaev, and A. Nylandsted Larsen, in *Proceedings of 23rd International Conference on the Physics of Semiconductors*, edited by M. Scheffler and R. Zimmermann (World Scientific, Singapore, 1996), Vol. 2, p. 1059.
[49] A. Barla, R. Rüffer, A. I. Chumakov, J. Metge, J. Plessel, and M. M. Abd-Elmeguid, Phys. Rev. B **61**, R14881 (2000).